nature medicine

Cancer cell–selective *in vivo* near infrared photoimmunotherapy targeting specific membrane molecules

Makoto Mitsunaga, Mikako Ogawa, Nobuyuki Kosaka, Lauren T Rosenblum, Peter L Choyke & Hisataka Kobayashi

Three major modes of cancer therapy (surgery, radiation and chemotherapy) are the mainstay of modern oncologic therapy. To minimize the side effects of these therapies, molecular-targeted cancer therapies, including armed antibody therapy, have been developed with limited success. In this study, we have developed a new type of molecular-targeted cancer therapy, photoimmunotherapy (PIT), that uses a target-specific photosensitizer based on a near-infrared (NIR) phthalocyanine dye, IR700, conjugated to monoclonal antibodies (mAbs) targeting epidermal growth factor receptors. Cell death was induced immediately after irradiating mAb-IR700–bound target cells with NIR light. We observed *in vivo* tumor shrinkage after irradiation with NIR light in target cells expressing the epidermal growth factor receptor. The mAb-IR700 conjugates were most effective when bound to the cell membrane and produced no phototoxicity when not bound, suggesting a different mechanism for PIT as compared to conventional photodynamic therapies. Target-selective PIT enables treatment of cancer based on mAb binding to the cell membrane.

Molecular-targeted cancer therapies have been developed to minimize the side effects of conventional cancer therapies such as surgery, radiation and chemotherapy. Among the existing targeted therapies, therapy with mAbs has the longest history, and, to date, over 25 therapeutic mAbs have been approved by the US Food and Drug Administration[1,2]. Effective mAb therapy traditionally depends on three mechanisms, antibody-dependent cellular cytotoxicity, complement-dependent cytotoxicity and receptor blockade, and requires multiple high doses of the mAb. mAbs have also been used at lower doses as vectors to deliver therapies such as radionuclides[3] and chemical or biological toxins[4]. Ultimately, however, dose-limiting toxicity affects the biodistribution and catabolism of the antibody conjugates.

Conventional photodynamic therapy (PDT), which combines a photosensitizing agent with the physical energy of non-ionizing light to kill cells, has been less commonly used for cancer therapy because the current nontargeted photosensitizers are also taken up in normal tissues, which causes serious side effects, although the excitation light itself is harmless in the NIR range (**Fig. 1**). Were it feasible to design a specifically targeted photosensitizer, the toxicity of this therapy could be greatly reduced. Although the targeted photosensitizer may distribute throughout the body, it is only active in areas where intense light is applied, which reduces the likelihood of off-target effects. Most existing photosensitizers are poorly selective small molecules that bind not only to cancer cells but also to normal cells, including the skin and other epithelial surfaces, resulting in unwanted phototoxicity. These agents are generally hydrophobic and therefore permeate into cells and produce reactive oxygen species intracellularly, leading to cell death. Thus, target-specific delivery of conventional photosensitizers is theoretically difficult because, after reaching the cell, the agent must still be internalized into organelles, for example, mitochondria, to be most effective. Various combinations of conventional photosensitizers and mAbs have been tested to improve their selectivity with limited success, especially when measured by *in vivo* therapeutic effects[5–11]. There are several reasons for these unsuccessful outcomes: (i) conventional photosensitizers have low extinction coefficients, meaning that they require conjugation of large numbers of photosensitizers to a single antibody molecule, potentially decreasing the binding affinity; (ii) conventional photosensitizers are mostly hydrophobic, leading to difficulties in conjugating photosensitizers to antibodies without compromising immunoreactivity and *in vivo* target accumulation; and (iii) conventional photosensitizers generally absorb light in the visible range, reducing tissue penetration.

In this study, we develop a mAb-based photosensitizer that is activated by NIR light for targeted PIT only when bound to the target molecule on the cancer cellular membrane. Further, because this agent also emits a diagnostic fluorescence, it can be used to direct the application of light to minimize exposure to nonrelevant tissues and to noninvasively monitor any therapeutic effects of excitation light.

RESULTS

In vitro characterization of mAb-IR700 conjugates

Conjugation of trastuzumab, an mAb directed against human epidermal growth factor receptor 2 (HER2), or panitumumab, an mAb

Molecular Imaging Program, Center for Cancer Research, National Cancer Institute, US National Institutes of Health, Bethesda, Maryland, USA. Correspondence should be addressed to H.K. (kobayash@mail.nih.gov).

Received 16 August 2010; accepted 22 March 2011; published online 6 November 2011; doi:10.1038/nm.2554

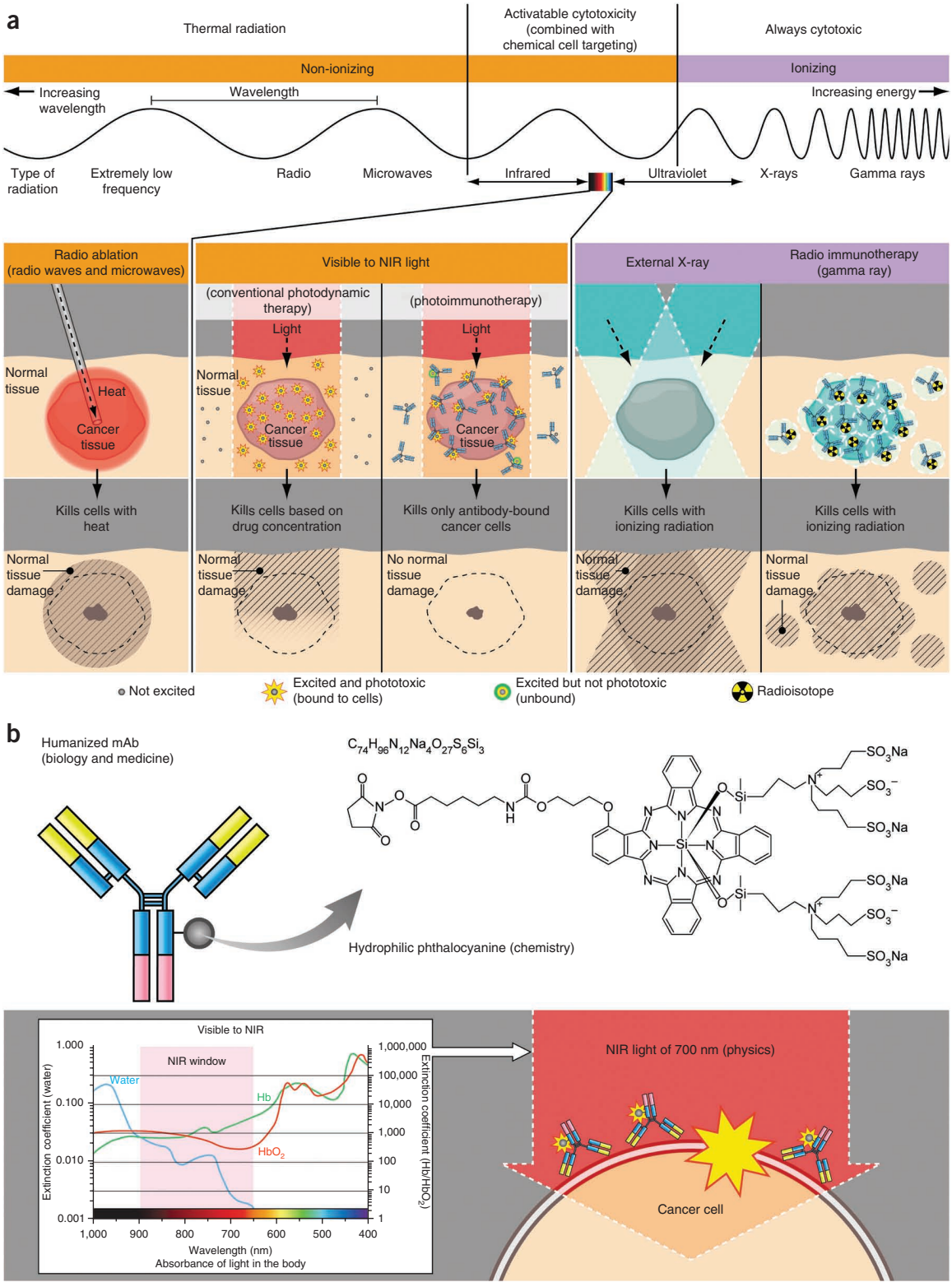

Figure 1 mAb-IR700 PIT in physics-based cancer therapies. (**a**) A schematic for explaining selective cancer therapy with PIT in the context of other physical cancer therapies that use electromagnetic wave irradiation. Although other physical cancer therapies induce different types of damages in the normal tissue, PIT targets cancer cells without damaging normal cells or tissues. (**b**) A schematic for explaining the photophysical, chemical and biological bases of PIT. From a biological and medicinal standpoint, humanized antibodies are used as a delivery vehicle for PIT therapy because of their high binding specificity, their accurate *in vivo* target delivery and their low immunogenicity among the clinically applicable targeting reagents. From a chemical standpoint, a hydrophilic phthalocyanine is used as an activatable cytotoxic 'nano-dynamite' reagent because of its high absorption of NIR light at 700 nm and the strong cytotoxicity induced only when associating with the cell membrane. From a physical standpoint, NIR light at 700 nm is used as an initiator for activating cytotoxicity because of its high energy among nonharmful nonionizing photons and its substantial *in vivo* tissue penetration.

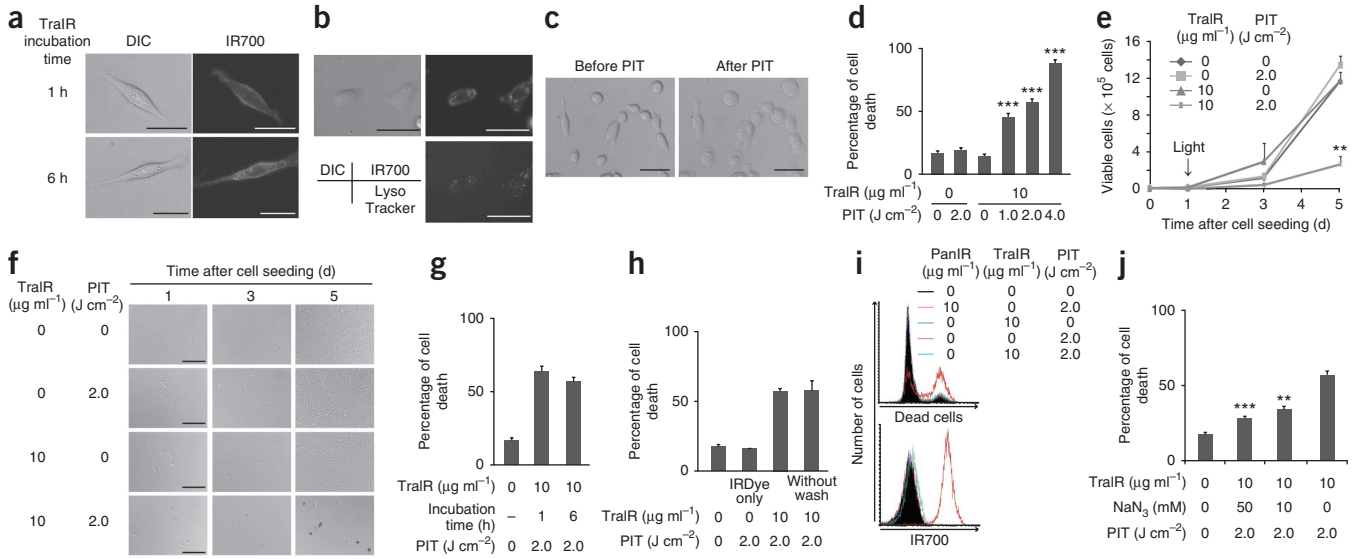

Figure 2 Target-specific cell death in response to Tra-IR700–mediated PIT in 3T3-HER2 cells. (**a**) Various subcellular localizations of Tra-IR700 (TraIR). Scale bars, 30 μm. (**b**) Lysosomal localization of Tra-IR700 6 h after incubation at 37 °C. Scale bars, 50 μm. (**c**) Microscopic observation of 3T3-HER2 cells before and after Tra-IR700–mediated PIT. Scale bars, 50 μm. (**d**) Irradiation dose-dependent and target-specific cell death in response to Tra-IR700–mediated PIT. Data are means ± s.e.m. ($n \geq 4$, $^{***}P < 0.001$ for treatment compared to untreated controls using a Student's *t* test). (**e**) Long-term growth inhibition in response to Tra-IR700–mediated PIT. Data are means ± s.e.m. ($n = 3$, $^{**}P < 0.01$ for treatment compared to untreated controls using a Student's *t* test). (**f**) Microscopic observation of growth inhibition in response to Tra-IR700–mediated PIT. Scale bars, 100 μm. (**g**) Internalization of Tra-IR700 was not required for phototoxic cell death. Data are means ± s.e.m. ($n = 3$). (**h**) Target-specific membrane binding of Tra-IR700 induced phototoxic cell death. Data are means ± s.e.m. ($n = 3$). (**i**) A431 cells negatively expressing HER2 did not show phototoxic effects after Tra-IR700–mediated PIT ($n = 3$). (**j**) Sodium azide (NaN_3) concentration–dependent inhibition of phototoxic cell death induced by Tra-IR700–mediated PIT. Data are means ± s.e.m. ($n = 3$, $^{**}P < 0.01$ $^{***}P < 0.001$, for treatment with 2.0 J cm^{-2} PIT and NaN_3 control compared to treatment and no NaN_3 control using a Student's *t* test). DIC, differential interference contrast; PanIR, Pan-IR700.

directed against human epidermal growth factor receptor 1 (HER1), to IRDye 700DX *N*-hydroxysuccinimide ester (IR700) resulted in approximately three IR700 molecules conjugated to each mAb molecule. The trastuzumab-IR700 (Tra-IR700) and panitumumab-IR700 (Pan-IR700) preparations showed strong association between mAbs and IR700 and contained no detectable mAb aggregates as determined by HPLC and SDS-PAGE (**Supplementary Fig. 1a**,**b**). We analyzed the *in vitro* immunoreactivity of the mAb-IR700 conjugates in a binding assay using ^{125}I-labeled mAb-IR700 conjugates and showed that 73.38% ± 0.39% (^{125}I–Tra-IR700) and 78.61% ± 0.89% (^{125}I–Pan-IR700) (mean ± s.d.) binding was achieved with each mAb conjugate, and we confirmed the specificity of the binding by blocking with excess native unconjugated mAb (nonspecific binding was less than 1.4%) (**Supplementary Fig. 1c**). Because the immunoreactivities of ^{125}I-Tra and ^{125}I-Pan measured using the same method were 78% ± 2% and 82% ± 3%, respectively, we confirmed minimal loss of mAbs with IR700 conjugation.

mAb-IR700 PIT leads to rapid necrotic cell death *in vitro*

We examined cytotoxicity studies of PIT primary targeting HER2 with Tra-IR700 (**Fig. 2**).We performed fluorescence microscopy to visualize the cellular binding locations of the conjugates. Consistent with previous studies, we detected IR700 fluorescence primarily on the cell surface of 3T3-HER2 cells, which express HER2, after incubation for 1 h at 4 °C with Tra-IR700, but we detected the fluorescence also inside the cells after incubation for 6 h at 37 °C with Tra-IR700, indicating a gradual internalization of Tra-IR700 (ref. 12) (**Fig. 2a**). Co-staining with LysoTracker Green showed colocalization of IR700 in the endolysosomal compartment (**Fig. 2b**). After incubation for either 1 h or 6 h with Tra-IR700, excitation light (from a fluorescence microscope at a power density of 2.2 mW cm^{-2}) induced fluorescence, cellular swelling, bleb formation and rupture of vesicles, indicating necrotic cell death (**Fig. 2c** and **Supplementary Video 1a**,**b**). We also observed necrotic cell death using HER1-positive A431 cells incubated with Pan-IR700, which we exposed to excitation light as described above (**Fig. 3**).

To further explore the nature of the phototoxicity of Tra-IR700 on 3T3-HER2 cells, we used a LIVE/DEAD cell viability assay to analyze acute phototoxicity and a trypan blue dye exclusion assay to analyze the effect of Tra-IR700 on proliferation. As cell death was induced

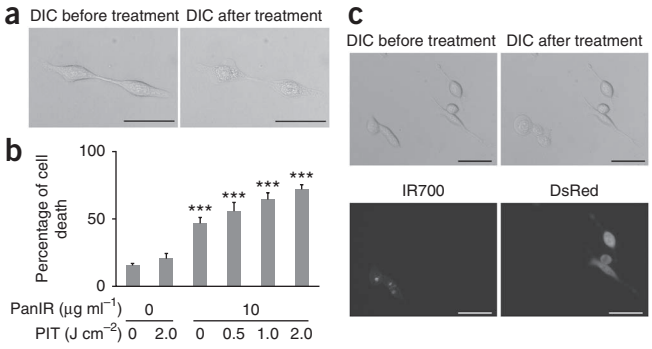

Figure 3 Target-specific cell death in response to Pan-IR700–mediated PIT in epidermal growth factor receptor (EGFR)-expressing A431 cells. (**a**) Microscopic observations before and after Pan-IR700–mediated PIT. Scale bars, 50 μm. (**b**) Irradiation dose-dependent and target-specific cell death in response to Pan-IR700–mediated PIT. Data are means ± s.e.m. ($n \geq 4$, $^{***}P < 0.001$ for treatment compared to untreated control using a Student's *t* test). (**c**) EGFR-expressing cell-specific necrotic cell death was induced by Pan-IR700–mediated PIT. Scale bars, 50 μm.

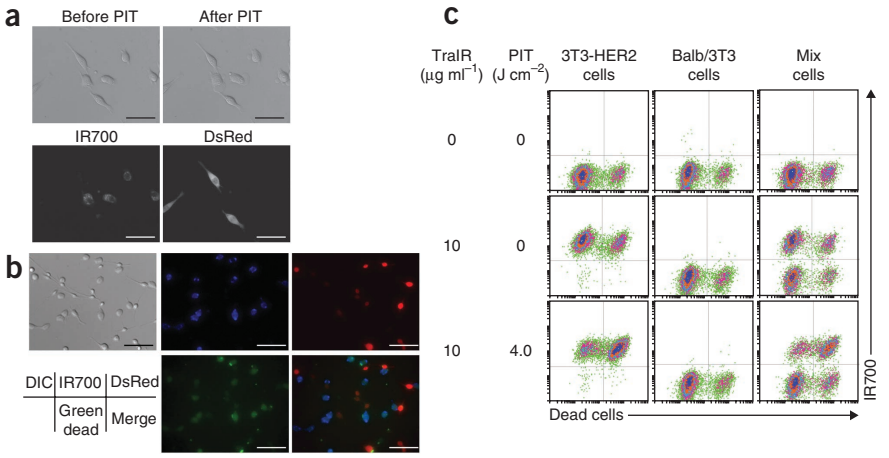

Figure 4 Tra-IR700–mediated PIT for co-cultured cells either expressing or not expressing HER2. (**a**) Induction of target-specific PIT leads to HER2-expressing cell–specific necrotic cell death. Scale bars, 50 μm (**Supplementary Video 2**). (**b**) HER2-specific cell death was confirmed using fluorescence microscopy with LIVE/DEAD cell viability Green staining. Scale bars, 100 μm. (**c**) Flow cytometric analysis for detecting HER2-specific cell death induced by Tra-IR700–mediated PIT. Shown are Tra-IR700–positive live cells (top left), Tra-IR700–positive dead cells (top right), Tra-IR700–negative live cells (bottom left) and Tra-IR700–negative dead cells (bottom right) ($n = 3$).

immediately after irradiation (**Supplementary Video 1a**,**b**), we performed a phototoxicity assay within 1 h after treatment. The percentage of cell death in target cells compared to untreated control cells was significantly influenced by the dose of excitation light (**Fig. 2d**). In addition, there was no significant cytotoxicity associated with exposure to Tra-IR700 alone in the absence of excitation light or with light exposure alone in the absence of Tra-IR700. We obtained similar results for A431 cells treated with Pan-IR700 (**Fig. 3b**); however, panitumumab alone had a noticeable treatment effect in A431 cells as a result of downregulation and signal inhibition of HER1 (ref. 13). Parental 3T3 cells served as HER2-receptor–negative controls, and, therefore, we chose 3T3-HER2 cells treated with Tra-IR700 for further *in vitro* study. A proliferation assay revealed that long-term growth inhibition was achieved only when cells were treated with Tra-IR700 and were also exposed to light (**Fig. 2e**,**f** and **Supplementary Fig. 2a**).

Phototoxicity induced only when mAb-IR700 is bound to the target

There was no significant difference in phototoxicity between 1 h and 6 h of incubation with Tra-IR700 (**Fig. 2g**), indicating that the membrane binding of Tra-IR700 was sufficient to induce cell death. When Tra-IR700 was localized to the endolysosomal compartment (**Fig. 2b**), it also induced rupture of the vesicle, with cellular swelling and bleb formation occurring after irradiation (**Supplementary Video 1a**). However, this did not appear to be a major cause of cell death, as we observed cell death without endolysosomal localization of Tra-IR700 within 1 h of incubation at 4 °C (**Supplementary Video 1b**). Notably, not washing the cells before irradiation did not influence the phototoxic effect, indicating that cellular membrane binding, and not just the presence of the conjugate, was key to the phototoxic effects of the conjugate. Further, the IR700 dye alone (200 nM, which is an equivalent concentration to that used for the Tra-IR700 conjugates described above) did not incorporate into the cells or induce phototoxicity (**Fig. 2h** and **Supplementary Fig. 2b**). Additionally, phototoxicity was blocked by the excess unconjugated trastuzumab in a dose-dependent manner (**Supplementary Fig. 2c**,**d**). Furthermore, Tra-IR700 did not induce a therapeutic effect in A431 cells (**Fig. 2i**). These results confirm that cell death is dependent on the specific membrane binding of Tra-IR700.

Reactive oxygen species (ROS) have been implicated in the cell death associated with conventional PDT. To clarify the role of photon-induced redox reactions (for example, singlet oxygen ($^1O_2$)) in producing phototoxicity with Tra-IR700 use, we added sodium azide (NaN_3)[14], (a redox quencher) to the medium when we irradiated the cells. Sodium azide partially decreased the percentage of cell death in a dose-dependent manner (**Fig. 2j**).

To confirm that the phototoxicity was target specific, we next treated 3T3-HER2 and Balb/3T3/DsRed cells, the latter of which is a parental HER2-negative Balb/3T3 cell line transfected with DsRed fluorescent protein, with Tra-IR700. Tra-IR700 was distributed in a HER2-specific manner and showed immediate cytotoxicity in 3T3-HER2 cells, whereas Balb/3T3/DsRed cells did not show phototoxicity after irradiation (**Fig. 4a** and **Supplementary Video 2**). In addition, LIVE/DEAD Green staining showed HER2-specific induction of cell death, as determined by multicolor fluorescence microscopy (**Fig. 4b**) and flow cytometry analysis (**Fig. 4c**). We also confirmed target-specific phototoxicity of Pan-IR700–mediated PIT in A431 cells and Balb/3T3/DsRed (HER1 negative) co-cultured cells (**Fig. 3c**). Overall, Tra-IR700 and Pan-IR700 showed identical therapeutic effects in HER2-positive (3T3-HER2) and HER1-positive (A431) cells, respectively, except for the fact that that unconjugated panitumumab showed noticeable growth inhibition, but unconjugated trastuzumab did not reduce growth with the dose we used.

Target-specific accumulation of mAb-IR700 *in vivo*

To examine the distribution of the mAb-IR700 conjugate *in vivo*, we prepared a xenograft tumor model that included mice with A431 (HER1 positive) and 3T3-HER2 (HER1 negative) tumors in each dorsum. We visualized the A431 tumors with IR700 fluorescence 1 d after intravenous injection of 50 μg of Pan-IR700 (**Fig. 5a**). The fluorescence intensity of Pan-IR700 in the A431 tumors decreased gradually over the 4 d after injection, whereas the tumor to background ratios (TBRs) increased during this period (**Fig. 5b**,**c**). The fluorescence intensity of the 3T3-HER2 tumor was the same as that of the background (non-tumor lesions). When we administered 300 μg of Pan-IR700 intravenously, the fluorescence intensity of the A431 tumor at 1 d after injection was more than three times higher than that resulting from a 50-μg injection; however, the TBR was lower because of the high intensity of the background signal (**Fig. 5b**,**c**). We found less antitumor activity in mice that received a 50-μg compared to a 300-μg injection of Pan-IR700 following irradiation (**Supplementary Fig. 3**), and, therefore, we chose the higher dose for use in the treatment study. We determined the biodistribution of Pan-IR700 using IR700 fluorescence because the amounts of radioactivity and fluorescence might be different in tissues as a result of their different excretion routes and catabolism when using dual-labeled radiolabeled Pan-IR700 (ref. 15). There was no other specific localization of IR700, except for accumulation in the bladder on day 1, probably as a result of the excretion of catabolized and unbound dye (**Fig. 5d** and **Supplementary Fig. 4a**).

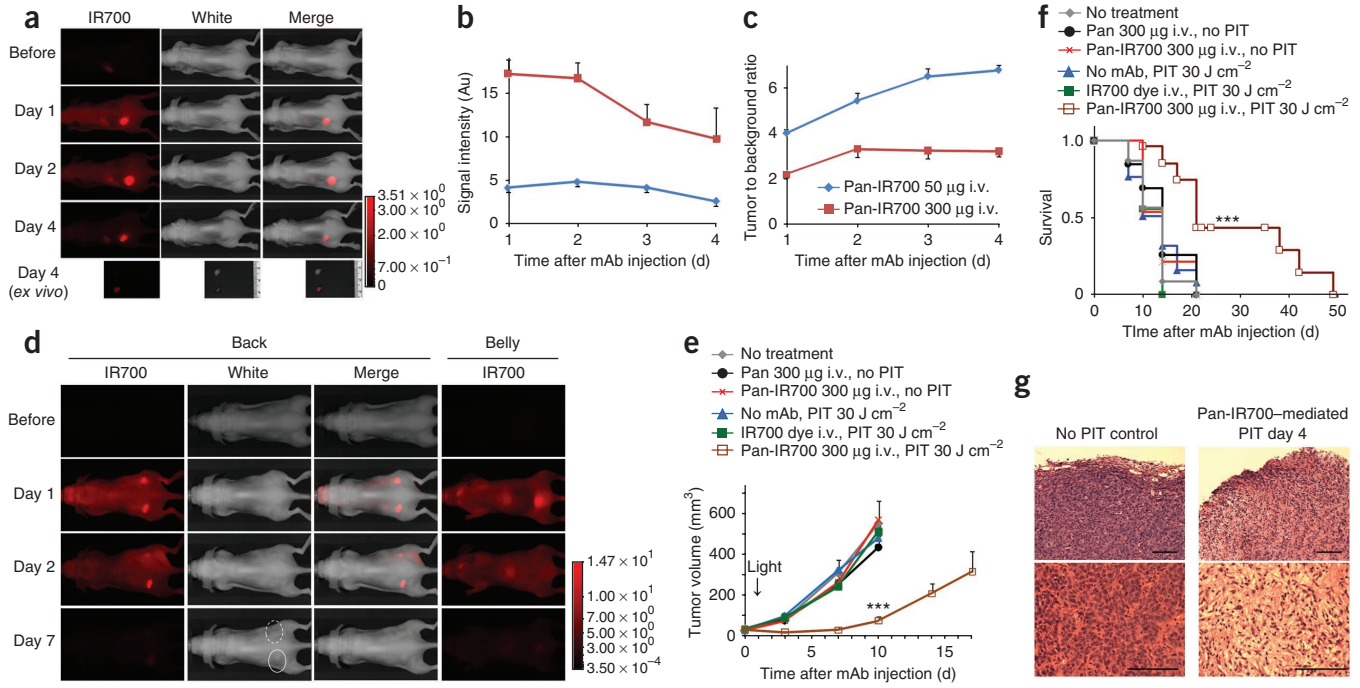

Figure 5 Pan-IR700–mediated PIT for HER1-expressing tumors *in vivo*. (**a**) HER1-positive A431 tumors (from the left dorsum) were selectively visualized as early as 1 d after injection with 50 μg of Pan-IR700. The HER1-negative 3T3-HER2 tumors (from the right dorsum) did not show detectable fluorescence ($n = 5$ mice). (**b**) The fluorescence intensity of IR700 in A431 tumors over time at two different doses of Pan-IR700. Data are means ± s.e.m. ($n = 4$ mice). (**c**) The TBR of the IR700 fluorescence intensity in A431 tumors over time at two different doses of intravenous (i.v.) Pan-IR700. Data are means ± s.e.m. ($n = 4$ mice). (**d**) The biodistribution of Pan-IR700. A431 tumors (from both sides of the dorsum) were selectively visualized with IR700 fluorescence as early as 1 d after injection with 300 μg of Pan-IR700. The right side of the tumor was irradiated with NIR light on day 1 after injection, and the left side of the tumor was covered with black tape. Tumor shrinkage was confirmed on day 7 after injection. Dashed line, irradiated tumor; solid line, nonirradiated tumor. (**e**) Target-specific tumor growth inhibition by Pan-IR700–mediated PIT in A431 tumors. PIT was performed on day 1 after injection with Pan-IR700 (corresponding to day 5 after tumor inoculation). Data are means ± s.e.m. ($n \geq 12$ mice in each group, $^{***}P < 0.001$ for treatment compared to the other control groups using a Kruskal-Wallis test with post-testing). (**f**) An analysis using a Kaplan-Meier survival curve of Pan-IR700–mediated PIT in A431 tumors ($n \geq 12$ mice in each group, $^{***}P < 0.001$ for treatment compared to the other control groups using a log-rank test with a Bonferroni's correction for multiplicity). (**g**) Histological observation of treated and untreated A431 tumors visualized using H&E staining ($n = 5$ mice). Scale bars, 100 μm. Pan, panitumumab.

mAb-IR700 PIT–induced target-specific tumor shrinkage

We treated A431 tumors with a single dose of light at 1 d after injection of Pan-IR700. We studied the efficacy of Pan-IR700–mediated PIT in eight groups of mice with A431 tumors ($n \geq 12$ mice in each group). All the tumors we treated had an area of less than 500 mm^3, as larger tumors were associated with side effects (for example, subcutaneous bleeding, tumor bleeding or a weakened state) that, in accordance with our institution's animal care and use guidelines, required that we kill the mice. Tumor volume was significantly reduced in A431 tumors treated with Pan-IR700–mediated PIT compared to untreated control mice (**Fig. 5e**), and survival was significantly prolonged in mice treated with Pan-IR700–mediated PIT compared to controls (**Fig. 5f**). We observed no significant therapeutic effect in any other control groups of mice without either one of the PIT components (mAb-IR700 injection or NIR light irradiation) (**Fig. 5e**,**f**). We observed similar results in 3T3-HER2 tumors treated with Tra-IR700–mediated PIT (**Supplementary Fig. 4b**). A pathological analysis revealed that only a few viable A431 tumor cells were present after Pan-IR700–mediated PIT, and we observed massive granulation with inflammatory change in the tumor nodule (**Fig. 5g**). We also observed that tissue edema developed superficially. To assess the acute phase toxicity of Pan-IR700, we repeatedly administrated 300 μg of Pan-IR700 intravenously twice a week for 4 weeks, but we observed no adverse effects at up to 8 weeks after treatment ($n = 4$) compared to the control group.

DISCUSSION

Conventional PDT for cancer therapy is based on the preferential accumulation of a photosensitizer in tumors to produce phototoxicity with minimal damage to surrounding tissue[16]. Traditionally, PDT is thought to be mediated by the generation of ROS, especially singlet oxygen, in the presence of oxygen[16]. However, because existing photosensitizers lack tumor selectivity, considerable damage occurs in normal tissues, which leads to dose-limiting toxicity. Thus, current methods of PDT would be improved if more selective targeting of the photosensitizer and more efficient phototoxicity per photon absorbed were possible.

Various combinations of conventional photosensitizers and mAbs have been tested to improve selectivity[5–11]. Although a large number of photosensitizers have been evaluated, IR700 has several favorable chemical properties. Amino-reactive IR700 is a relatively hydrophilic dye that can be covalently conjugated with mAb using the *N*-hydroxysuccinimide ester of IR700, which leads to high tumor uptake. IR700 also has a more than fivefold higher extinction coefficient (2.1×10^5 $M^{-1}cm^{-1}$ at the absorption maximum of 689 nm)[17] than conventional photosensitizers such as the hematoporphyrin derivative Photofrin (1.2×10^3 $M^{-1}cm^{-1}$ at 630 nm), the meta-tetrahydroxyphenylchlorin Foscan (2.2×10^4 $M^{-1}cm^{-1}$ at 652 nm) and the mono–L-aspartylchlorin e6 NPe6/Laserphyrin (4.0×10^4 $M^{-1}cm^{-1}$ at 654 nm)[18].

The selectivity of mAb-IR700 is derived from its activation after binding to the cell membrane of target cells; unbound conjugate does not contribute to phototoxicity. Our short-term viability assays, as well as long-term proliferation assays, showed that this conjugate was capable of inducing specific cell death. When we treated co-cultures of receptor-positive and receptor-negative cells, only the receptor-positive cells were killed, despite the presence of unbound mAb-IR700 in the culture medium. This selective cell killing minimizes damage to normal cells.

Although the mechanism of the phototoxicity of mAb-IR700 is not completely clear, the agent must be bound to the cellular membrane to be active. Treatment with sodium azide, a well-known redox quencher and singlet oxygen scavenger, only partially reduced the phototoxicity but did not totally eliminate the effectiveness of the conjugate. This indicates that ROS generation is a minor part of the phototoxic effect. That phototoxicity was induced after 1 h of incubation with mAb-IR700 at 4 °C indicates that internalization of the conjugate is not required for its activity. This differs from the current generation of PDT agents that require intracellular localization to be effective. Video microscopy showed rapid visible damage to the membrane and lysosomes after exposure to light after incubation for more than 6 h at 37 °C, at which time the mAb conjugate was internalized. Previous studies have indicated that intracellular uptake of mAb-photosensitizer conjugates is responsible for inducing phototoxicity[6–10]. Although this new mAb-IR700 conjugate does not require internalization for phototoxic cell death, cell-surface antigen binding is required. For example, the rupture of the endolysosome occurred within a second of exposure to light. Cell death induced by singlet oxygen generally induces a slower apoptotic cell death (**Supplementary Fig. 5a**,**b**)[19,20]. Because cell membrane damage was so quickly induced even at 4 °C by this method, we hypothesize that the cell death was caused by the rapid expansion of locally heated water, with relatively minor effects being caused by singlet oxygen[21].

Another desirable feature of PIT using fluorescent mAb-IR700 conjugate is that it permitted the detection of targeted tissue. Theoretically, this would allow specific lesions to be identified with PIT rather than needing to irradiate the entire field. The doses required for diagnosis (50 μg), however, were substantially lower than those required for therapy (300 μg). Improved intratumoral distribution of the antibody occurred at the therapeutic dose (**Supplementary Fig. 6**)[22,23]. Because both bound and unbound agents fluoresce, there is a relatively high background signal at therapeutic doses. Nevertheless, after PIT, the fluorescence of the treated tumors decreased and eventually disappeared, suggesting a potential means of monitoring the treatment.

One difficulty in interpreting the *in vivo* results of this study is that trastuzumab, but not panitumumab, showed minor therapeutic effects by itself without the application of light. Because panitumumab is an IgG2 and trastuzumab is an IgG1, this effect was probably mediated by the effects of antibody-dependent cellular cytotoxicity and complement-dependent cytotoxicity, even though we administered nonsaturating doses of each[24]. On the basis of the similarity of the phototoxicity induced with three different mAbs against several different cells expressing various numbers of respective target molecules, and considering the potentially additive benefits from immunotherapy (**Supplementary Fig. 7**), we believe that this method may be generally applicable to other mAbs[25,26].

The NIR light excitation wavelength (peaking at 689 nm) allows a penetration of at least several centimeters into tissues[16]. By using fiber-coupled laser diodes with diffuser tips, NIR light can be delivered to within several centimeters of otherwise inaccessible tumors located deep under the body surface. Using such fibers, PDT has been used to treat brain tumors and the peritoneal metastasis of ovarian cancer[27]. In addition to treating solid cancers, it may be possible to target circulating tumor cells using this method, as they can be excited when they traverse superficial vessels. Although we observed no toxicity in our experiments, clinical translation of this method will require formal toxicity studies. In addition, free IR700 and catabolized IR700 are readily excreted into urine within 1 h after administration without accumulating in any specific organ (**Supplementary Fig. 8**). The other component of PIT, light irradiation with NIR at 690 nm, is unlikely to be toxic except at thermal doses. Theoretically, there should be no limitations on the cumulative irradiation dose of NIR light, unlike with ionizing radiation such as X-rays or gamma rays. Therefore, repeated PIT might be possible for long-term treatment of some patients with cancer. Repeated PIT with three different regimens (three or four fractionated NIR irradiations with a single dose of mAb-IR700 or four cycles of PIT every 2 weeks after multiple doses of antibody) controlled tumor regrowth, resulting in tumor-free survival at more than 4 months.

In conclusion, we developed a target-specific PIT based on the mAb-IR700 conjugate. The photosensitizer IR700 is excited in the NIR range, leading to deeper tissue penetration that results in successful eradication of subcutaneously xenografted tumors after only a single dose of external NIR light irradiation. Targeted phototoxicity seems to be primarily dependent on binding of mAb-IR700 to the cell membrane and, to a lesser extent, on internalization and ROS formation. The ability to covalently conjugate any number of different antibodies to IR700 means that this may be a highly flexible theranostic platform. The fluorescence induced by the conjugate can be used to noninvasively guide PIT and monitor the results of therapy. Thus, the mAb-IR700 conjugate is a promising therapeutic and diagnostic agent for the treatment of cancer.

METHODS

Methods and any associated references are available in the online version of the paper at http://www.nature.com/naturemedicine/.

Note: Supplementary information is available on the Nature Medicine website.

ACKNOWLEDGMENTS

This research was supported by the Intramural Research Program of the US National Institutes of Health, National Cancer Institute, Center for Cancer Research. We would like to thank C. Regino, T. Hirano and C. Paik for their technical support.

AUTHOR CONTRIBUTIONS

M.M. conducted experiments, performed analysis and wrote the manuscript. M.O., N.K. and L.T.R. conducted experiments and performed analysis. P.L.C. wrote the manuscript and supervised the project. H.K. planned and initiated the project, designed and conducted experiments, wrote the manuscript and supervised the project.

COMPETING FINANCIAL INTERESTS

The authors declare no competing financial interests.

Published online at http://www.nature.com/naturemedicine/.
Reprints and permissions information is available online at http://www.nature.com/reprints/index.html.

1. Waldmann, T.A. Immunotherapy: past, present and future. *Nat. Med.* **9**, 269–277 (2003).
2. Reichert, J.M., Rosensweig, C.J., Faden, L.B. & Dewitz, M.C. Monoclonal antibody successes in the clinic. *Nat. Biotechnol.* **23**, 1073–1078 (2005).
3. Goldenberg, D.M., Sharkey, R.M., Paganelli, G., Barbet, J. & Chatal, J.F. Antibody pretargeting advances cancer radioimmunodetection and radioimmunotherapy. *J. Clin. Oncol.* **24**, 823–834 (2006).
4. Pastan, I., Hassan, R., Fitzgerald, D.J. & Kreitman, R.J. Immunotoxin therapy of cancer. *Nat. Rev. Cancer* **6**, 559–565 (2006).

5. Mew, D., Wat, C.K., Towers, G.H. & Levy, J.G. Photoimmunotherapy: treatment of animal tumors with tumor-specific monoclonal antibody-hematoporphyrin conjugates. *J. Immunol.* **130**, 1473–1477 (1983).
6. Sobolev, A.S., Jans, D.A. & Rosenkranz, A.A. Targeted intracellular delivery of photosensitizers. *Prog. Biophys. Mol. Biol.* **73**, 51–90 (2000).
7. Carcenac, M. *et al.* Internalisation enhances photo-induced cytotoxicity of monoclonal antibody-phthalocyanine conjugates. *Br. J. Cancer* **85**, 1787–1793 (2001).
8. Vrouenraets, M.B. *et al.* Development of meta-tetrahydroxyphenylchlorin-monoclonal antibody conjugates for photoimmunotherapy. *Cancer Res.* **59**, 1505–1513 (1999).
9. Vrouenraets, M.B. *et al.* Targeting of aluminum (III) phthalocyanine tetrasulfonate by use of internalizing monoclonal antibodies: improved efficacy in photodynamic therapy. *Cancer Res.* **61**, 1970–1975 (2001).
10. Hamblin, M.R., Miller, J.L. & Hasan, T. Effect of charge on the interaction of site-specific photoimmunoconjugates with human ovarian cancer cells. *Cancer Res.* **56**, 5205–5210 (1996).
11. Mew, D. *et al.* Ability of specific monoclonal antibodies and conventional antisera conjugated to hematoporphyrin to label and kill selected cell lines subsequent to light activation. *Cancer Res.* **45**, 4380–4386 (1985).
12. Ogawa, M., Regino, C.A., Choyke, P.L. & Kobayashi, H. *In vivo* target-specific activatable near-infrared optical labeling of humanized monoclonal antibodies. *Mol. Cancer Ther.* **8**, 232–239 (2009).
13. Yang, X.D. *et al.* Eradication of established tumors by a fully human monoclonal antibody to the epidermal growth factor receptor without concomitant chemotherapy. *Cancer Res.* **59**, 1236–1243 (1999).
14. Pooler, J.P. & Valenzeno, D.P. The role of singlet oxygen in photooxidation of excitable cell membranes. *Photochem. Photobiol.* **30**, 581–584 (1979).
15. Ogawa, M. *et al.* Dual-modality molecular imaging using antibodies labeled with activatable fluorescence and a radionuclide for specific and quantitative targeted cancer detection. *Bioconjug. Chem.* **20**, 2177–2184 (2009).
16. Dougherty, T.J. *et al.* Photodynamic therapy. *J. Natl. Cancer Inst.* **90**, 889–905 (1998).
17. Wilson, B.C. & Patterson, M.S. The determination of light fluence distributions in photodynamic therapy. in *Photodynamic therapy of neoplastic disease*, Vol. 1 (ed. Kessel, D.) 129–144 (CRC Press, Boca Raton, Florida, USA, 1990).
18. Detty, M.R., Gibson, S.L. & Wagner, S.J. Current clinical and preclinical photosensitizers for use in photodynamic therapy. *J. Med. Chem.* **47**, 3897–3915 (2004).
19. Weishaupt, K.R., Gomer, C.J. & Dougherty, T.J. Identification of singlet oxygen as the cytotoxic agent in photoinactivation of a murine tumor. *Cancer Res.* **36**, 2326–2329 (1976).
20. Patterson, M.S., Madsen, S.J. & Wilson, B.C. Experimental tests of the feasibility of singlet oxygen luminescence monitoring *in vivo* during photodynamic therapy. *J. Photochem. Photobiol. B* **5**, 69–84 (1990).
21. Thorpe, W.P., Toner, M., Ezzell, R.M., Tompkins, R.G. & Yarmush, M.L. Dynamics of photoinduced cell plasma membrane injury. *Biophys. J.* **68**, 2198–2206 (1995).
22. Kosaka, N. *et al.* Semiquantitative assessment of the microdistribution of fluorescence-labeled monoclonal antibody in small peritoneal disseminations of ovarian cancer. *Cancer Sci.* **101**, 820–825 (2010).
23. Kosaka, N. *et al.* Microdistribution of fluorescently-labeled monoclonal antibody in a peritoneal dissemination model of ovarian cancer. *Proc. SPIE* **7576**, 757604 (2010).
24. Mandler, R., Kobayashi, H., Hinson, E.R., Brechbiel, M.W. & Waldmann, T.A. Herceptin-geldanamycin immunoconjugates: pharmacokinetics, biodistribution, and enhanced antitumor activity. *Cancer Res.* **64**, 1460–1467 (2004).
25. Nanus, D.M. *et al.* Clinical use of monoclonal antibody HuJ591 therapy: targeting prostate specific membrane antigen. *J. Urol.* **170**, S84–S88 (2003).
26. van Dongen, G.A., Visser, G.W. & Vrouenraets, M.B. Photosensitizer-antibody conjugates for detection and therapy of cancer. *Adv. Drug Deliv. Rev.* **56**, 31–52 (2004).
27. Zhong, W. *et al. In vivo* high-resolution fluorescence microendoscopy for ovarian cancer detection and treatment monitoring. *Br. J. Cancer* **101**, 2015–2022 (2009).

ONLINE METHODS

Cells. *HER2*-gene–transfected NIH3T3 (3T3-HER2) cells and A431 cells expressing HER1 were used for PIT. As a control, Balb/3T3 cells that express DsRed fluorescent protein but that do not express HER1 or HER2 (Balb/3T3/DsRed) were used. Cells were grown in RPMI 1640 supplemented with 10% FBS and 1% penicillin-streptomycin in tissue culture flasks in a humidified incubator at 37 °C in an atmosphere of 95% air and 5% carbon dioxide.

Fluorescence microscopy. To detect the antigen-specific localization of IR700, fluorescence microscopy was performed with a BX51 or IX81 fluorescence microscope (Olympus America). Detailed conditions and settings are described in the **Supplementary Methods**.

***In vitro* photoimmunotherapy.** 3T3-HER2 or A431 cells were seeded into 35 mm cell-culture dishes and incubated at 37 °C for 24 h. The medium was then replaced with fresh culture medium containing 10 μg ml^{-1} of Tra-IR700 or Pan-IR700 and was then incubated for either 6 h at 37 °C or for 1 h at 4 °C. After washing with PBS, phenol red–free culture medium was added. Cells were then irradiated with light from a red-light–emitting diode at wavelengths of 670–690 nm (FluorVivo (INDEC Systems)) and a power density of 2.6 mW cm^{-2}, as measured with an optical power meter (PM 100 (Thorlabs)).

Phototoxicity assay. The cytotoxic effect of PIT mediated by Tra-IR700 or Pan-IR700 was determined with a LIVE/DEAD Fixable Green Dead Cell Stain Kit (Invitrogen). After treatment, 3T3-HER2 or A431 cells were trypsinized and washed with PBS. Green fluorescent reactive dye was added in the cell suspension and incubated at 18–25 °C for 30 min. Cells were then analyzed on a flow cytometer (FACSCalibur, BD BioSciences).

Proliferation assay. Cells were seeded into 35-mm cell culture dishes at a density of 1×10^4 cells per dish. The day after seeding, the cells were treated using PIT either mediated or not mediated by Tra-IR700. Cell viability was determined by a trypan blue dye exclusion assay at 1, 3 and 5 d after cell seeding. Viable cells for the treated group and the untreated controls were counted on a hemacytometer after trypsinization. The growth of the cells in each group was also photographed under a microscope (IX81, Olympus America) at each time point.

Biodistribution study. All *in vivo* procedures were conducted in compliance with the Guide for the Care and Use of Laboratory Animal Resources (1996), US National Research Council, and approved by the National Cancer Institute/NIH Animal Care and Use Committee. Six-week-old to 8-week-old female homozygote athymic nude mice were purchased from Charles River (National Cancer Institute Frederick). During treatment, mice were anesthetized with isoflurane. One million A431 cells were injected subcutaneously in the left dorsum of each mouse. Four days after cell injection, either 50 μg or 300 μg of Pan-IR700 was administered intravenously. To confirm the antigen-specific localization of the Pan-IR700, 1×10^6 3T3-HER2 cells were injected subcutaneously in the right dorsum of each mouse at the same time as the injection of the A431 cells. Fluorescence images were obtained at each indicated time point with a Pearl Imager (LI-COR Biosciences) using a 700-nm fluorescence channel. Regions of interest for both the tumor and the background were placed to obtain equivalent sized areas containing the same number of pixels. TBRs were calculated using the following formula: TBR = ((mean tumor intensity) – (mean background intensity)) / ((mean non-tumor intensity) – (mean background intensity)).

***In vivo* photoimmunotherapy.** To determine tumor volume, the greatest longitudinal diameter (length) and the greatest transverse diameter (width) from each tumor were determined using an external caliper. Each tumor's volume, based on the caliper measurements, was calculated using the following formula: tumor volume = length × $width^2 \times 0.5$ (ref. 28). Four days after the injection of A431 cells, tumors whose volume reached approximately 40 mm^3 were selected for the study. Animals were randomized into eight groups of at least 12 animals per group for the following treatments: (i) no treatment; (ii) 300 μg of panitumumab injected intravenously without PIT; (iii) 300 μg of Pan-IR700 injected intravenously without PIT; (iv) PIT performed at 30 J cm^{-2} without Pan-IR700; (v) free IR700 dye at a dose equivalent to 300 μg of Pan-IR700 injected intravenously and PIT performed at 30 J cm^{-2}; (vi) 50 μg of Pan-IR700 injected intravenously and PIT performed at 30 J cm^{-2}; (vii) 50 μg of Pan-IR700 and 250 μg of panitumumab injected intravenously and PIT performed at 30 J cm^{-2}; or (viii) 300 μg of Pan-IR700 injected intravenously and PIT performed at 30 J cm^{-2}. After treatment, the mice were monitored daily and their tumor volume was measured twice a week until it reached 500 mm^3, at which time mice were killed with carbon dioxide gas. To test short-term toxicity, 300 μg of Pan-IR700 was repeatedly administrated intraveneously in mice without tumors twice a week for 4 weeks.

Statistical analyses. Statistical analyses were carried out using the statistics program GraphPad Prism (GraphPad Software). Details are described in the **Supplementary Methods**.

Additional methods. Detailed methodology is described in the **Supplementary Methods**.

28. Euhus, D.M., Hudd, C., LaRegina, M.C. & Johnson, F.E. Tumor measurement in the nude mouse. *J. Surg. Oncol.* **31**, 229–234 (1986).

doi:10.1038/nm.2554